Electronic Supporting Information for:

Effect of the 1D / 2D Dimensionality in Copper and Silver Thiolate Coordination Polymers on their Photophysical Properties

Oleksandra Veselska,[a,b] Ahmad Abdallah,[a] Alexis Giraudon,[a,c] Chloé Andrade,[a,d] Saly Hawila,[a] Nathalie Guillou,[e] Erwann Jeanneau,[f] Miguel Monge,[g] Adel Mesbah,[a] Alexandra Fateeva,[h] Stéphane Pailhès,[d] Gilles Ledoux,[d] Florent Perret,[c] Aude Demessence*[a]

a. Université Claude Bernard Lyon 1, CNRS, IRCELYON, UMR 5256, Villeurbanne 69100, France

b. Czech Technical University in Prague, Institute of Experimental and Applied Physics, Prague 11000, Czech Republic

c. Université Claude Bernard Lyon 1, CNRS, INSA, CPE, ICBMS, UMR 5246, Villeurbanne 69622, France

d. Université Claude Bernard Lyon 1, CNRS, ILM, UMR 5306, Villeurbanne 69100, France

e. Université Versailles Saint-Quentin-en-Yvelines, Université Paris-Saclay, CNRS, ILV, UMR 8180, Versailles 78035, France

f. Université Claude Bernard Lyon 1, CNRS, Centre de Diffractométrie Henri Longchambon, Villeurbanne 69622, France

g. Departamento de Química, Instituto de Investigación en Química (IQUR), Complejo Científico Tecnológico, Universidad de La Rioja, Logroño 26004, Spain

h. Université Claude Bernard Lyon 1, CNRS, LMI, UMR 5615, Villeurbanne 69100, France

* aude.demessence@ircelyon.univ-lyon1.fr

Characterization techniques

Structure determination

Single-crystal X-ray data of [Cu(*m*-SPhCO$_2$H)]$_n$ **1** were collected at the CRISTAL beamline at Synchroton Soleil, using a set-up adapted for small crystals at 100.0(1) K on a four-circle diffractometer equipped with an Atlas CCD detector. Data reduction was performed using CrysAlisPro. [1] An empirical absorption correction [2, 3] was applied using spherical harmonics on the basis of multiple scans of equivalent reflections, implemented in SCALE3 ABSPACK scaling algorithm. The structure was determined by direct methods using the SIR97 program[4] combined with Fourier difference syntheses and refined against F using all reflections by using the CRYSTALS program.[5] All atomic displacement parameters for non-hydrogen atoms were refined with anisotropic terms. Hydrogen atoms were theoretically located on the basis of the conformation of the supporting atom or taking account the presence of potential hydrogen bonds. Hydrogen atoms have then been refined by using the riding model. CCDC-1906390 contains the supplementary crystallographic data. X-ray crystallographic data and refinement details are summarized in the table S1.

High resolution **powder X-ray** diffraction data of [Ag(*m*-SPhCO$_2$H)]$_n$ **2**, [Cu(*m*-SPhCO$_2$Me)]$_n$ **3** and [Ag(*m*-SPhCO$_2$Me)]$_n$ **4** were collected on the CRISTAL beamline at Soleil Synchrotron (Gif-sur-Yvette, France). A monochromatic beam was extracted from the U20 undulator beam by means of a Si(111) double monochromator. The wavelengths (Table S1) were refined from a LaB_6 (NIST Standard Reference Material 660a) powder diagram recorded prior to the experiment. The samples were loaded in a 0.7 mm capillary (Borokapillaren, GLAS, Schönwalde, Germany) mounted on a spinner rotating at about 5 Hz to improve the particles' statistics. Diffraction data were collected in continuous scanning mode with a MYTHEN2 X 9K detector (Dectris) allowing a measurement in less than 5 minutes. Calculations of structural investigations of **2**, **3** and **4** were performed with the TOPAS (indexing, charge flipping, simulated annealing, difference Fourier calculations, Rietveld refinement).[6] For **2**, the LSI-indexing method converged to a monoclinic unit cell very similar to that of **1** (Table S1)**,** with satisfactory figure of Merit M_{20} = 19. Systematic extinctions were consistent with the $P2_1/n$ space group, which was used to initialize the structural determination by simulated annealing. Indexing of **3** and **4** is more questionable. Indeed, the diffraction patterns of **4** show differences

from one synthesis to another showing that the structural model of **4** is more complicated than the proposed one. Powder pattern of **3** could be indexed in the orthorhombic unit cell in the *Pnn*2 space group, but peaks are very broad, and the very large *a* parameter of the unit cell makes it difficult to determine the *c* one. Nevertheless, given the similarity between the observed and calculated patterns, the 1D nature of **3** and **4** is not questionable and the proposed structural models could be considered as a good approximation to the real ones.

Routine PXRD. Routine X-ray diffraction was carried out on a Bruker D8 Advance A25 diffractometer using Cu Kα radiation equipped with a 1-dimensional position-sensitive detector (Bruker LynxEye). X-Ray scattering was recorded between 4° and 90° (2θ) with 0.02° steps and 0.5 s per step (28 min for the scan). Divergence slit was fixed to 0.2° and the detector aperture to 189 channels (2.9°).

SEM. SEM images were obtained with FEI Quanta 250 FEG scanning electron microscope, samples were mounted on stainless pads and coated with carbon to prevent charging during observation.

FTIR. The infrared spectra were obtained from a Bruker Vector 22 FT-IR spectrometer with KBr pellets at room temperature and registered from 4000 cm^{-1} to 400 cm^{-1}.

TGA. Thermo-gravimetric analyses were performed with a TGA/DSC 1 STARe System from Mettler Toledo. Around 5 mg of sample was heated at a rate of 10 °C.min^{-1}, in a 70 μL alumina crucible, under air (20 mL.min^{-1}).

Elemental analysis. Sulphur percentage is determined by full combustion at 1320-1360 °C under O_2 stream and analysis of SO_2 and is titrated in a coulometric-acidimetric cell. Carbon and hydrogen percentages are determined by full combustion at 1030-1070 °C under O_2 stream and transformed into CO_2 and H_2O and are titrated on a coulometric detector. Analysis precision is 0.3% absolute for carbon, sulfur and hydrogen.

UV-vis. UV-vis absorption spectra were carried out with a LAMBDA 365 UV/Vis Spectrophotometer from Perkin Elmer in solid state at room temperature.

Photoluminescence excitation and emission spectra measurements. For those compounds used for photophysical studies, PXRD was always measured to exclude impurities.

The photoluminescence measurements were performed on a homemade apparatus. The sample was illuminated by an EQ99X laser driven light source filtered by a Jobin Yvon Gemini 180 monochromator. The exit slit from the monochromator was then reimaged on the sample by two 100m focal length, 2 inch diameter MgF_2 lenses. The whole apparatus has been calibrated by means of a Newport 918D Low power calibrated photodiode sensor over the range 190-1000 nm. The resolution of the system being 4 nm. The emitted light from the sample is collected by an optical fibre connected to a Jobin-Yvon TRIAX320 monochromator equipped with a cooled CCD detector. At the entrance of the monochromator different long pass filter can be chosen in order to eliminate the excitation light. The resolution of the detection system is 2 nm.

Temperature control over the sample was regulated with a THMS-600 heating stage with T95-PE temperature controller from Linkam Scientific Instruments.

Luminescence lifetime measurements. Luminescence lifetime measurements were excited with a diode pumped 50Hz tunable OPO laser from EKSPLA. The luminescence from the sample was collected with an optical fibre and afterwards filtered by a long pass filter (FEL550 from Thorlabs) and fed to a R2949 photomultiplier tube from Hamamatsu. Photon arrival times were categorized by the MCS6A multichannel scaler from Fast ComTec.

The coinage metal thiolates are known to exhibit complex multicomponent lifetime decays [7-9]. In this study, we limit our lifetime decay data treatment to the estimation of its half-life, $t_{1/2}$, by identifying the time when half of the photons is emitted. And the mean lifetime, τ, was calculated from half-life as:

$$\tau = \frac{t_{1/2}}{\ln(2)}$$

Quantum yield measurements. Quantum yield measurements of solid samples at RT for compounds were performed using a Hamamatsu Quantaurus-QY C11347-11 integrating sphere. QY was registered by performing a scan measurement for each sample in the 300-450 nm range every 10 nm to account for the difference in the excitation wavelength maxima of four compounds. The maximal QY values were obtained for **1** (1.3 %) at 410 nm, for **2** (0.5 %) at 360 nm, for **3** (9.1 %) at 350 nm, for **4** (4.5 %) at 380 nm.

Synthesis of coordination polymers

Chemicals. *meta*-mercaptobenzoic acid (or *m*-$HSPhCO_2H$, > 97.0 %) was purchased from TCI. Copper (II) chloride dihydrate ($CuCl_2 \cdot 2H_2O$, ≥ 99 %), hydrochloric acid (HCl, 37 %, ACS reagent), sulfuric acid (H_2SO_4, 95-97 %) were purchased from Sigma Aldrich. Silver (I) nitrate ($AgNO_3$, > 99 %) was purchased from Alfa Aesar. Ethanol, acetone and dimethylformamide (DMF) were purchased from VWR Chemicals. All reagents and solvents were used as received.

Synthesis of the ligand (*m*-$HSPhCO_2Me$): In a 3-necks round bottom flask, *m*-$HSPhCO_2H$ (2 g, 13 mmol) was dissolved in 70 mL of degassed anhydrous methanol. 1 mL of 90% H_2SO_4 was added and reaction was let to proceed under gentle reflux overnight until total reactant consumption. Methanol was evaporated and 100 mL of ethyl acetate was added to the reaction mixture, this organic phase was washed three times with saturated $NaHCO_3$ solution. After drying on $MgSO_4$, the organic phase was concentrated to afford quantitatively *m*-$HSPhCO_2Me$. ^1H NMR (300mHZ, $CDCl_3$): d(ppm) 7.846 (1H, d J=1.53 Hz, H_a), 7.846 (1H, dd J=1.53 Hz and 7.74Hz, H_b), 7.733 (1H, d= 7.77Hz, H_c), 7.199 (1H, dd J=7.77 Hz and 7.74Hz, H_d). ^{13}C NMR (300mHZ, $CDCl_3$): d(ppm) 166.370 (C=O), 133.394 (C-Aro), 131.772 (C-Aro), 131.010 (C-Aro), 130.132 (C-Aro), 129.062 (C-Aro), 126.735 (C-Aro), 52.264 (CH_3). ESI-MS (positive mode): 169.0 ($M + H^+$), 191.0 ($M + Na^+$).

Synthesis of [Cu(*m*-$SPhCO_2H$)]$_n$ (1): 1 mL of 0.1 M HCl was added to 5 mL of aqueous solution of $CuCl_2 \cdot 2H_2O$ (75 mg, 0.44 mmol, 1 eq.) followed by the addition of a solution of *m*-$HSPhCO_2H$ (192 mg, 1.25 mmol, 2.8 eq.) in DMF (5 mL). The reaction was let to proceed for 18 h at 120 °C in a 20 ml sealed vial. The obtained product was washed with 40 mL of ethanol for 3 times. It was recovered by centrifugation at 4000 rpm and dried in air. The obtained pale-yellow solid is not soluble in any solvent, it is formed of pellet-like crystals suitable for single crystal XRD. Yield: 85 % (84 mg). Chemical Formula: $C_7H_5CuO_2S$. Molecular Weight: 216.72. CuO content from TGA (calc.) wt%: 36.9 (36.7).

Synthesis of [Ag(*m*-$SPhCO_2H$)]$_n$ (2): 10 mL of aqueous solution of $AgNO_3$ (100 mg, 0.59 mmol, 1 eq.) was added to *m*-$HSPhCO_2H$ (91 mg, 0.59 mmol, 1 eq.). The reaction was let to proceed for 18 h at 120 °C in a 20 ml sealed vial. The product was obtained and washed with 40 mL of ethanol for 3 times. It was recovered by centrifugation at 4000 rpm and was dried in air.

The obtained white powder is not soluble in any solvent, it contains no crystals suitable for single crystal XRD. Yield: 54 % (83 mg). Chemical Formula: $C_7H_5AgO_2S$. Molecular Weight: 261.05. Silver content from TGA (calc.) wt%: 42.2 (41.3).

Synthesis of [Cu(*m*-SPhCO$_2$Me)]$_n$ (3): 5 mL of $CuCl_2 \cdot 2H_2O$ (63 mg, 0.37 mmol) solution in DMF was added to 5 mL solution of *m*-HSPhCO$_2$Me (86.86 mg, 72.26 µL, 0.514 mmol) in DMF, followed by the addition of 1 mL of H_2SO_4 (1 M). The reaction was let to proceed for 24 h at 120 °C in a 20 ml sealed vial. The obtained product was washed and filtered with ethanol for 3 times, and with acetone for 3 times. It was then dried in air. The yellow solid is not soluble in any solvent, it is formed of very thick rod-like crystals which are unsuitable for single crystal XRD. Yield: 69 % (39.8 mg). Chemical Formula: $C_8H_7CuO_2S$. Molecular Weight: 230.75. Elemental analysis (calc.) wt%: C, 37.27 (41.2); H, 3.34 (3.06); S, 14.11 (13.9); O, 18.18 (13.87). CuO content from TGA (calc.) wt%: 35.2 (34.5).

Synthesis of [Ag(*m*-SPhCO$_2$Me)]$_n$ (4): 5 mL of aqueous solution of $AgNO_3$ (100 mg, 0.59 mmol) was added to 5 mL of aqueous solution of *m*-HSPhCO$_2$Me (99.71 mg, 82.9 µL, 0.59 mmol). The reaction was let to proceed for 24 h at 120 °C in a 20 ml sealed vial. The obtained product was washed and filtered with ethanol for 3 times, and with acetone for 3 times. It was then dried in air. The yellow solid is not soluble in any solvent, it is formed of very thick rod-like crystals which are unsuitable for single crystal XRD. Yield: 21 % (34.7 mg). Chemical Formula: $C_8H_7AgO_2S$. Molecular Weight: 275.07. Elemental analysis (calc.) wt%: C, 35.33 (34.93); H, 2.39 (2.56); S, 11.76 (11.66); O, 11.93 (11.63). Silver content from TGA (calc.) wt%: 41.4 (39.2).

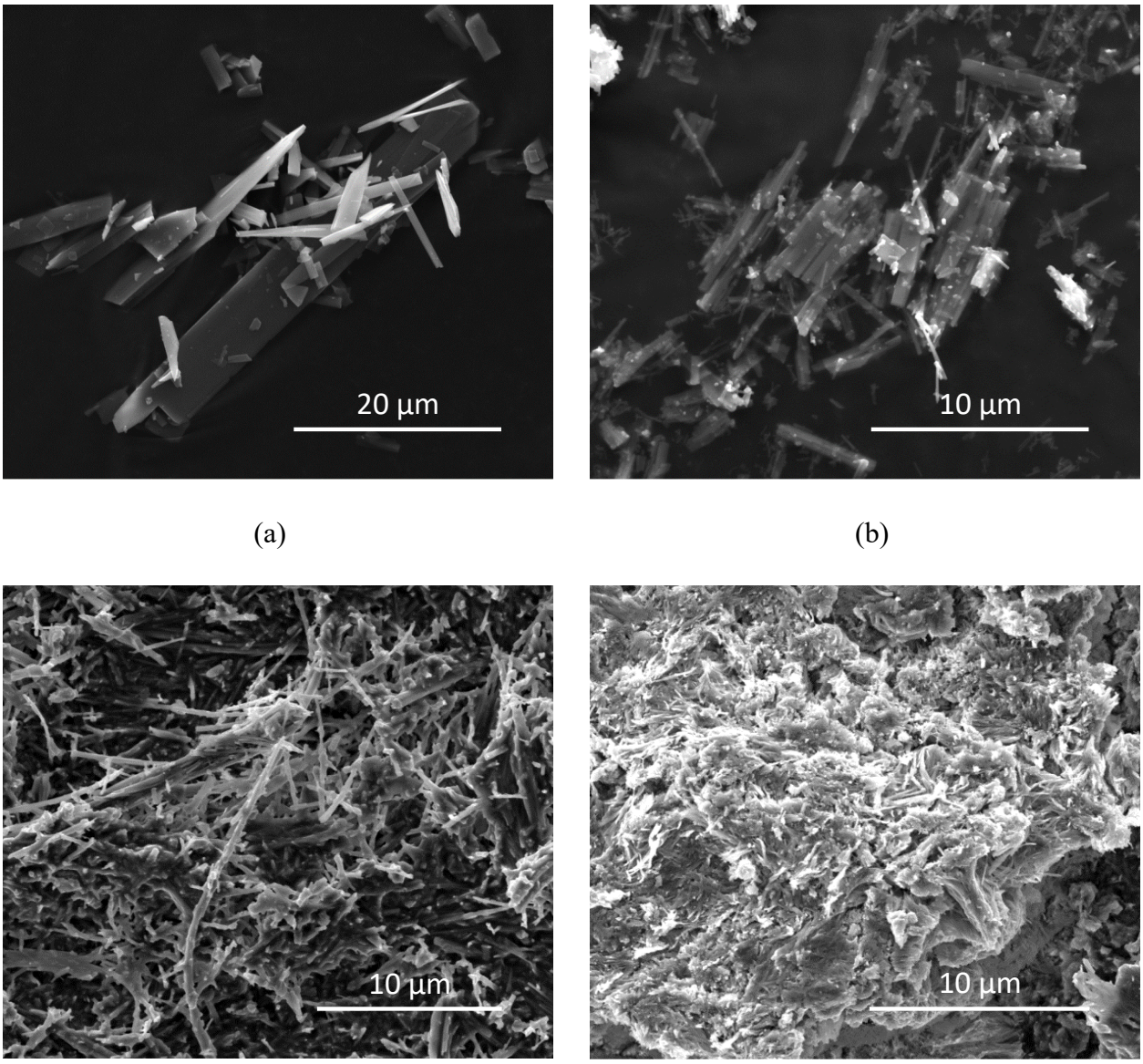

Figure S1. SEM images of (a) **1**, (b) **2**, (c) **3** and (d) **4**.

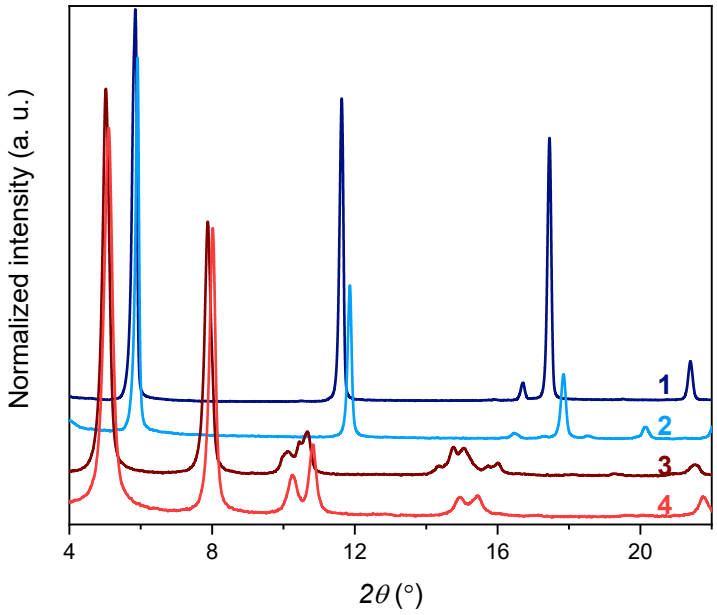

Figure S2. Zoom on the low angles PXRD patterns of **1** (dark blue), **2** (blue), **3** (dark red) and **4** (red).

Table S1. Crystallographic data and Rietveld refinement parameters for **1**, **2**, **3** and **4**.

	Compound 1	**Compound 2**	**Compound 3**	**Compound 4**
Data	single crystal	powder	powder	powder
Empirical formula	$C_7H_5Cu_1O_2S_1$	$C_7H_5Ag_1O_2S_1$	$C_8H_7Cu_1O_2S_1$	$C_8H_7Ag_1O_2S_1$
M_r	216.73	261.05	230.72	275.05
Crystal system	Monoclinic	Monoclinic	Orthorhombic	Orthorhombic
Space group	*P* $2_1/n$	*P* $2_1/n$	*P n n* 2	*P n n* 2
a (Å)	3.9047(2)	4.5017(6)	34.723(6)	34.348(8)
b (Å)	30.438(3)	5.4687(6)	11.844(2)	11.611(2)
c (Å)	5.6182(4)	29.799(2)	3.993(2)	4.377(2)
β (°)	91.933(4)	93.70(2)	-	-
V (Å^3)	667.35(8)	732.1(2)	1642.2(6)	1745.6(8)
Z	4	4	8	8
λ (Å)	0.67173	0.7289	0.6714	0.6714
Number of reflections	2574	758	316	292
Structural parameters	105	11	12	13
R[$F^2 > 2\sigma(F^2)$]	0.1001	-	-	-
wR(F^2) or R_B	0.1324	0.032	0.043	0.036
GoF	0.9993	11.20	8.13	16.33
R_p/R_{wp}	-	0.058/0.066	0.047/0.056	0.076/0.095

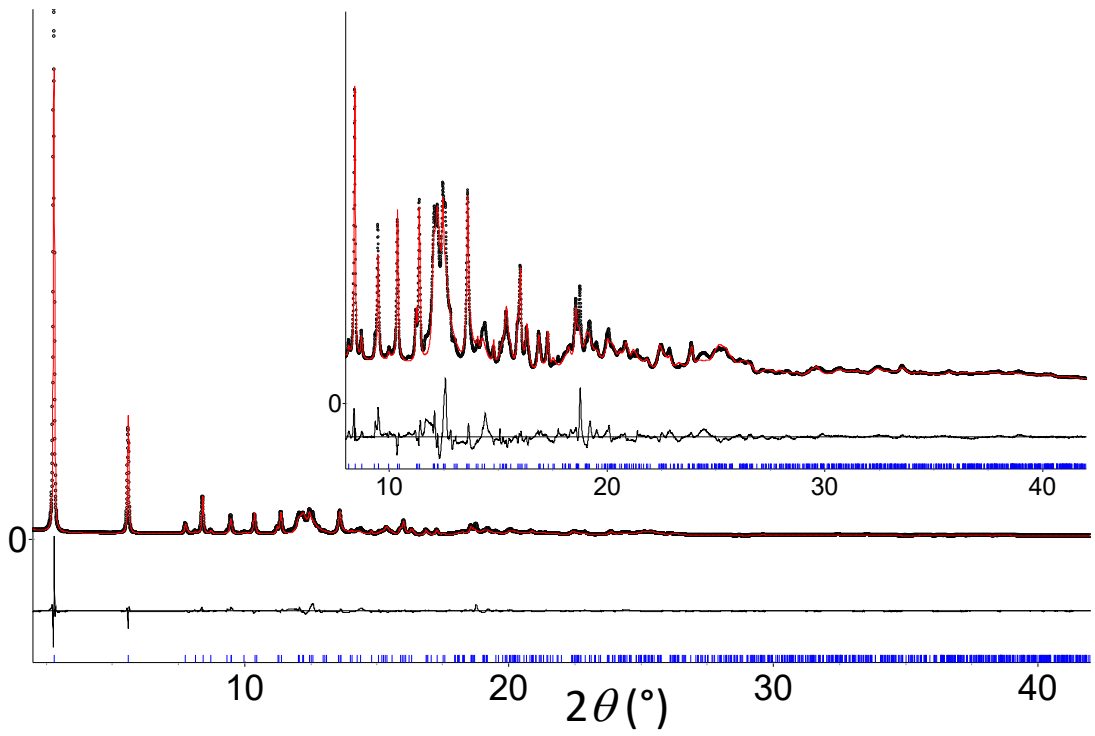

(a)

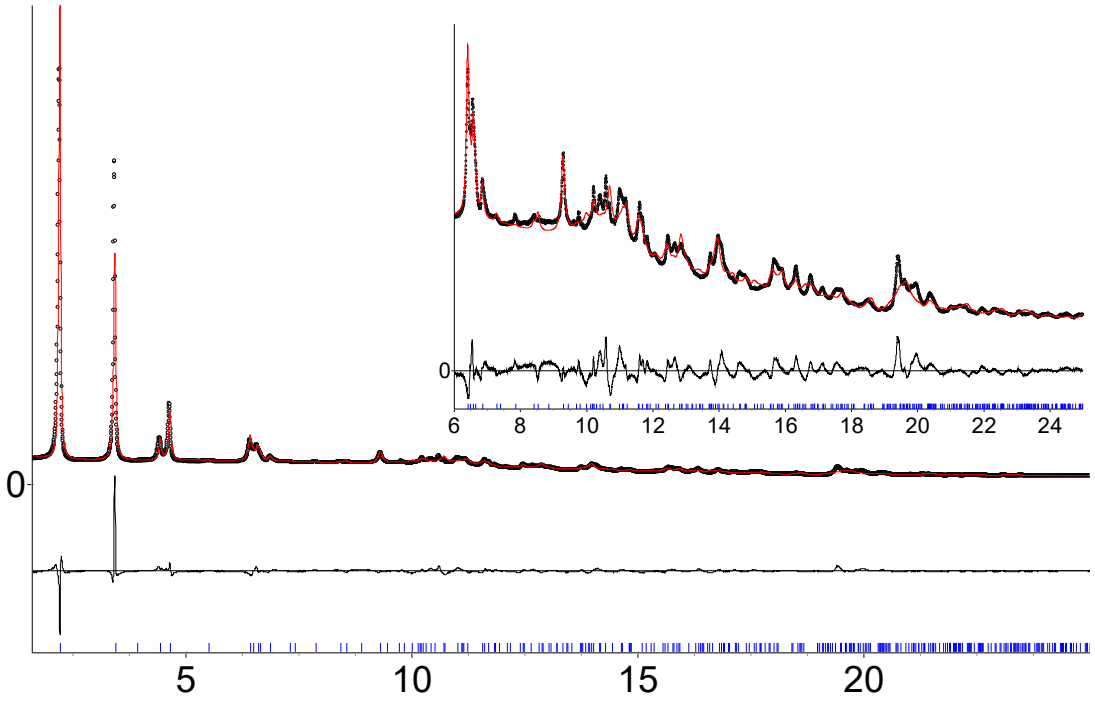

(b)

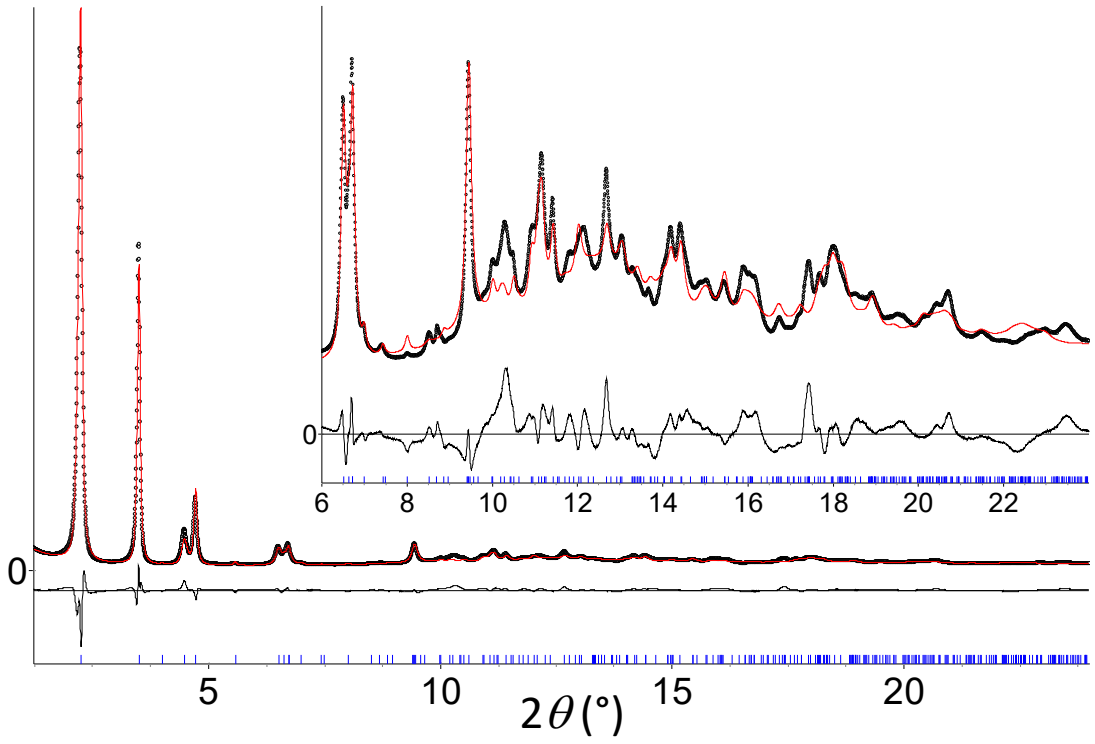

(c)

Figure S3. Final Rietveld plots of (a) **2**, (b) **3** and (c) **4** showing observed (black dots), calculated (red line), and difference (black line) curves. A zoom at high angles is shown as inset.

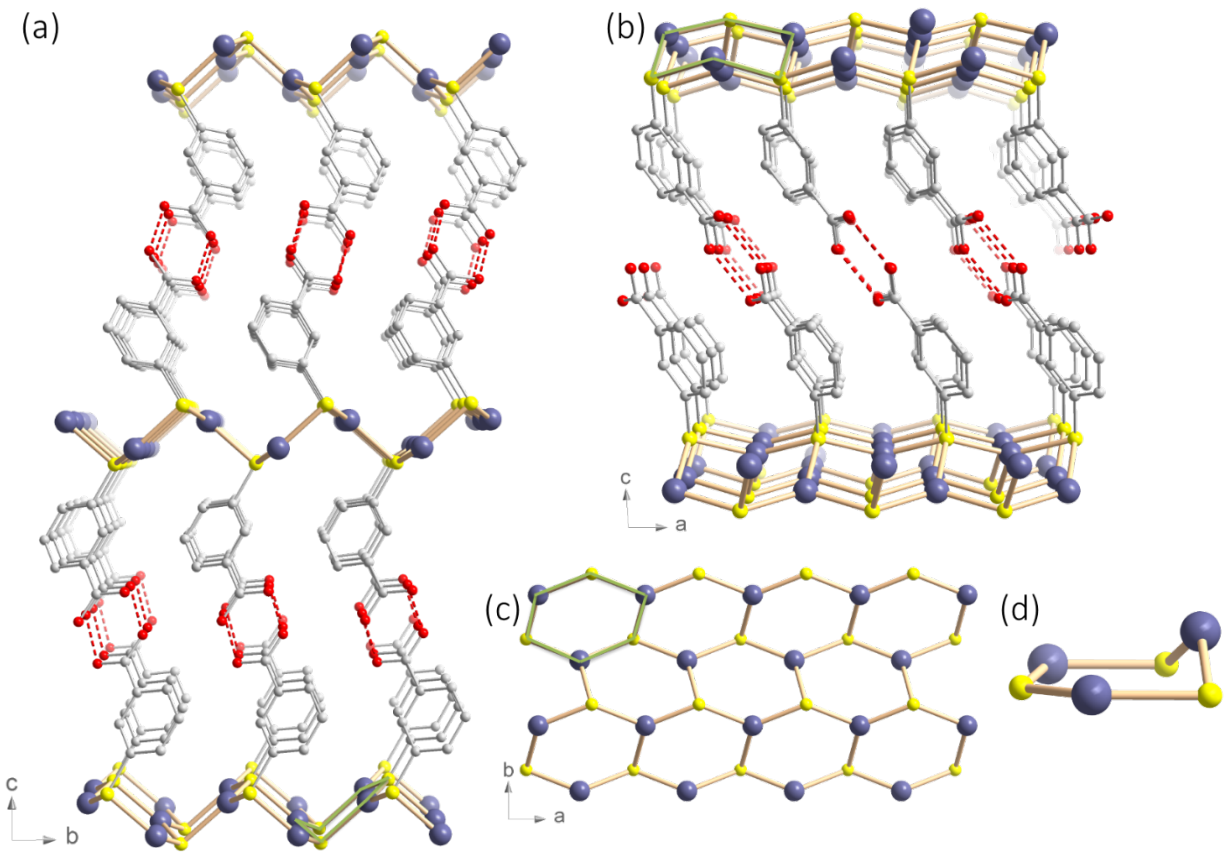

Figure S4. Structure of **2**: (a) view of the 2D lamellar structure along *a* axis and (b) *b* axis, (c) view of the Ag-S layer in the *(ab)* plane, (d) view of Ag_3S_3 hexagon, it is shown with green lines in (a) and (b). Blue, Ag; yellow, S; red, O; grey, C. Hydrogen atoms are omitted. Red dashed lines represent the hydrogen bonds.

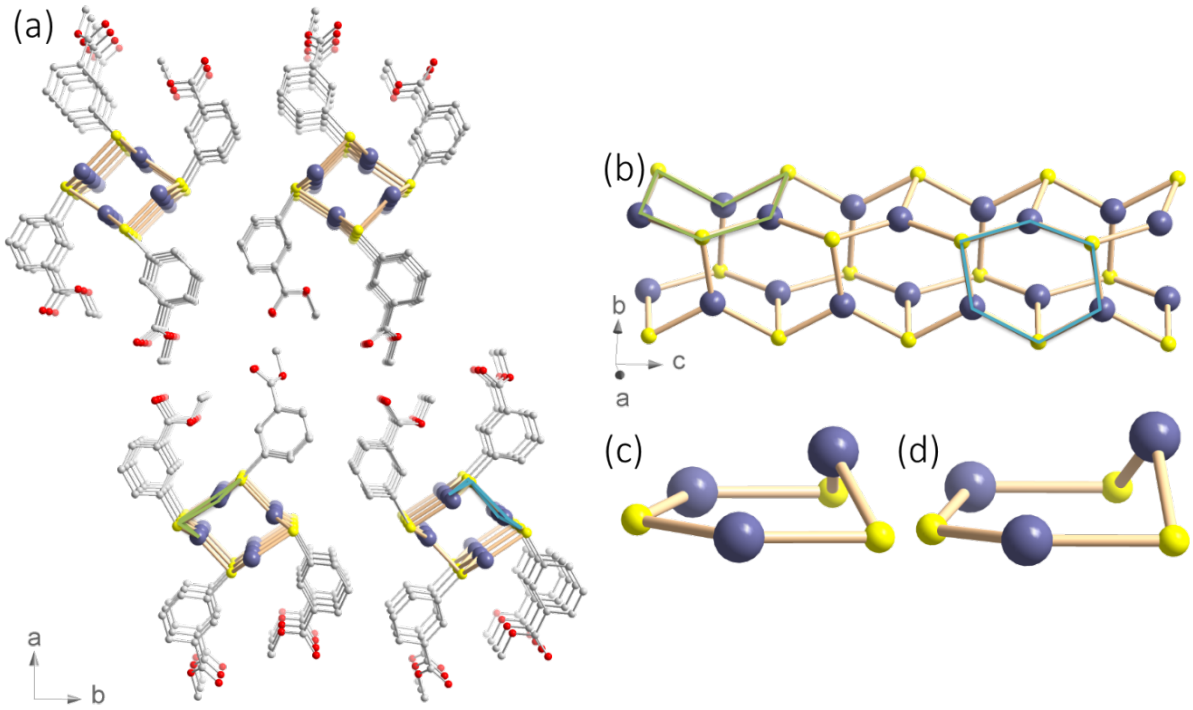

Figure S5. Structure of **4**: (a) view of the 1D columnar structure along *c* axis and (b) Ag-S column, (c) and (d) view of Ag_3S_3 hexagons, they are shown with green and blue lines, respectively, in (a) and (b). Blue, Ag; yellow, S; red, O; grey, C. Hydrogen atoms are omitted.

Table S2. Selected distances and angles for compounds **1**, **2**, **3** and **4**, as well as for some previously published copper and silver thiolate CPs.

Structural type	Compound	M-S, Å	M-M, Å	S-M-S, °	M-S-M, °	Dihedral angle in M_3S_3, °	π-π, Å	Ref.
2D layers (half-chair hexagons)	**[Cu(*m*-SPhCO$_2$H)]$_n$ Compound 1**	2.242(2) 2.244(2) 2.294(2)	3.494(1)† 3.599(2)† 3.905(1)†	116.3(1) 121.0(1) 121.1(1)	100.7(1) 105.0(1) 121.0(1)	118.7(1)	3.905(1)	This work
	[Ag(*m*-SPhCO$_2$H)]$_n$ Compound 2	2.456(9) 2.518(6) 2.528(9)	3.450(4)† 3.978(4)† 4.502(4)†	105.7(3) 124.6(3) 129.2(4)	104.1(3) 124.6(3) 129.2(4)	104.8(4)	4.50(2)	This work
	[Cu(*p*-SPhOH)]$_n$	2.252(4) 2.253(3)	3.238(5)† 3.450(5)† 4.001(4)†	112.9(1) 121.9(1) 125.3(1)	91.9(1) 100.0(1) 125.3(1)	103.2(2)	4.001(1)	[10]
	[Cu(*p*-SPhCO$_2$Me)]$_n$	2.244(3) 2.255(3) 2.282(4)	3.313(3)† 3.492(3)† 3.966(3)†	114.0(2) 122.2(2) 123.6(2)	93.8(2) 101.0(2) 123.6(2)	106.5(1)	3.966(1)	[11]
2D layers (distorted boat hexagons)	**[Cu(*p*-SPhCO$_2$H)]$_n$**	2.243(3) 2.290(2) 2.302(3)	3.030(2)† 3.519(2)†	104.1(1) 126.0(1) 129.8(1)	83.6(1) 101.9(1) 116.4(1)	-	5.77(2)	[7]
	[Ag(*p*-SPhCO$_2$H)]$_n$	2.456(4) 2.493(4) 2.623(4)	2.936(2)† 3.687(2)†	97.2(2) 126.4(2) 131.3(2)	70.5(1) 96.3(2) 118.2(2)	-	5.82(1)	[8]
	[Ag(*p*-SPhCO$_2$Me)]$_n$	2.437(5) 2.489(5) 2.627(5)	2.973(3)† 3.653(2)†	97.0(2) 124.4(2) 132.3(2)	71.8(2) 95.7(2) 120.2(2)	-	5.91(2)	[8]
1D columns	**[Cu(*m*-SPhCO$_2$Me)]$_n$ Compound 3**	2.25(2) 2.26(7) 2.37(7) 2.42(2) 2.42(5) 2.43(5)	2.74(1) 2.97(5)† 2.98(5)† 3.49(4)† 3.50(4)† 3.99(9)† 4.32(2)	108.3(8) 109.7(8) 111(2) 115.8(5) 118.1(5) 119(3)	77.1(6) 78.7(6) 96.3(7) 96.8(7) 110(3) 119(3)	65.5(8) 101.6(8) 129.9(8) 142.9(8)	4.00(7)	This work
	[Ag(*m*-SPhCO$_2$Me)]$_n$ Compound 4	2.47(4) 2.47(2) 2.49(3) 2.49(4) 2.63(5)	2.96(2)† 3.38(2) 3.39(2)† 3.45(2)† 3.83(2)† 3.98(2) 4.38(3)†	111.9(7) 113.0(7) 117(2) 122.5(7) 124(1) 129.6(8)	72.9(7) 86.3(9) 87.9(6) 97.2(7) 117(3) 124(1)	68.4(7) 83.7(8)	4.38(5)	This work
	[Cu(*o*-SPhCO$_2$Me)]$_n$	2.250(5) 2.299(4) 2.362(4) 2.369(4)	2.900(4)† 3.058(4)† 3.506(3) 3.556(3)†	115.41(2) 118.13(2) 120.15(2) 120.84(2)	76.91(2) 79.58(2) 96.76(2) 100.40(2)	64.0(5) 109(1)	4.04(8)	[12]

		2.395(4) 2.401(4)	3.607(4)† 3.848(3)† 4.040(4)†	121.33(2) 121.96(2)	120.15(2) 121.96(2)			
	[Ag(*o*-SPhCO$_2$Me)]$_n$	2.504(5) 2.525(5) 2.565(4) 2.597(5) 2.635(5) 2.638(5)	3.083(3)† 3.203(3)† 3.341(3) 3.940(3) 4.091(2)† 4.481(2)†	102.70(2) 111.56(2) 120.41(2) 123.12(2) 124.28(2) 134.44(2)	71.55(1) 77.75(2) 80.67(1) 104.84(2) 120.41(2) 124.28(2)	62.2(4) 85(1)	4.48(1)	[12]
	[Cu(*o*-SPhCO$_2$H)]$_n$	2.261(5) 2.285(5) 2.400(5)	3.048(4)† 3.276(5) 3.962(3)†	117.4(2) 118.3(2) 121.3(2)	81.1(2) 81.6(2) 121.3(2)	74.7(3)	3.96(2)	[9]
	[Ag(*o*-SPhCO$_2$H)]$_n$	2.486(8) 2.561(8) 2.641(7)	3.296(4)† 3.442(5) 4.434(3)†	114.8(3) 117.4(3) 122.9(3)	78.5(3) 79.8(2) 122.9(3)	70.2(3)	4.434(13)	[9]
	[Cu(SMe)]$_n$	2.228(8) 2.285(2)	3.00(1)† 3.16(1) 4.01(1)†	115.0(1) 128.0(1)	83.4(1) 128.0(1)	76.7(1)	-	[13]
	[Cu(SPh)]$_n$	2.270(2) 2.298(2) 2.303(2)	2.965(3)† 3.437(3)† 3.593(5) 3.268(3)†	112.9(1) 113.6(1) 133.5(1)	80.0(1) 97.6(1) 113.6(1)	88.5(3)	3.827(2)	[14]
	[Cu(*p*-SPhMe)]$_n$	2.247(4) 2.248(4) 2.249(4) 2.252(4)	2.923(1)† 2.948(4)† 2.973(5) 2.983(4)† 3.132(5)† 3.296(5) 4.030(4)†	112.7(1) 114.7(2) 115.6(1) 118.5(2) 127.4(1)	81.9(1) 83.0(1) 88.2(1) 127.4(1)	74.5(2) 83.3(2)	4.030(3)	[14]
	[Cu(*p*-SPhOMe)]$_n$	2.249(4) 2.250(1) 2.250(3) 2.251(2)	2.75(5)† 2.83(5) 2.93(5)† 3.31(4)† 3.28(4)† 3.56(6) 4.15(2)†	100.8(4) 106.1(7) 119.3(5) 121.8(5) 134.6(4)	75.3(5) 81.4(5) 93.6(6) 94.9(6) 134.7(6)	83(2) 84(2)	4.153(2)	[14]

†bridged by sulfur atoms.

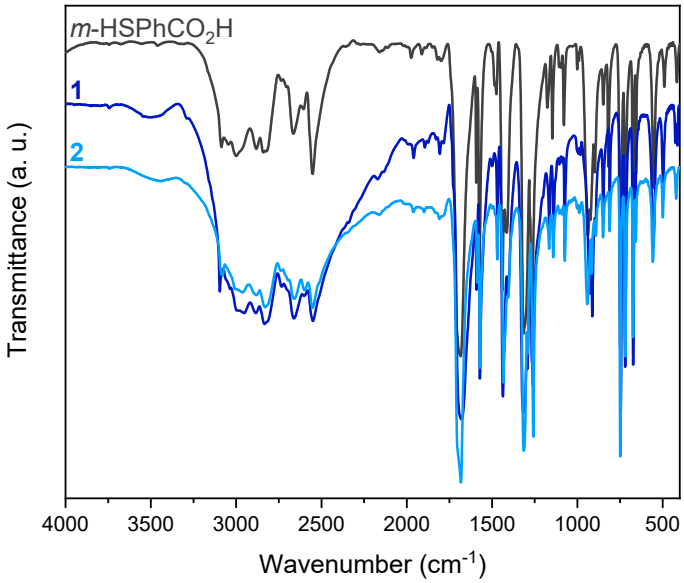

(a)

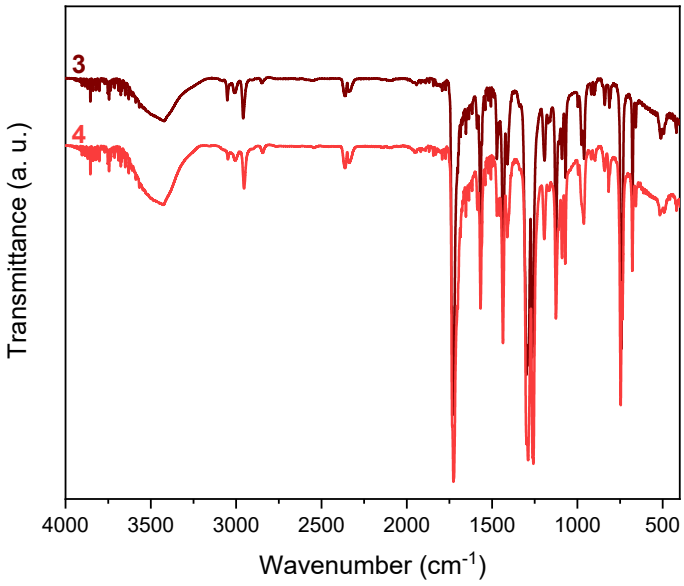

(b)

Figure S6. FT-IR spectra of (a) *m*-HSPhCO2H (dark grey), **1** (dark blue), **2** (blue), and (b) **3** (dark red), **4** (red).

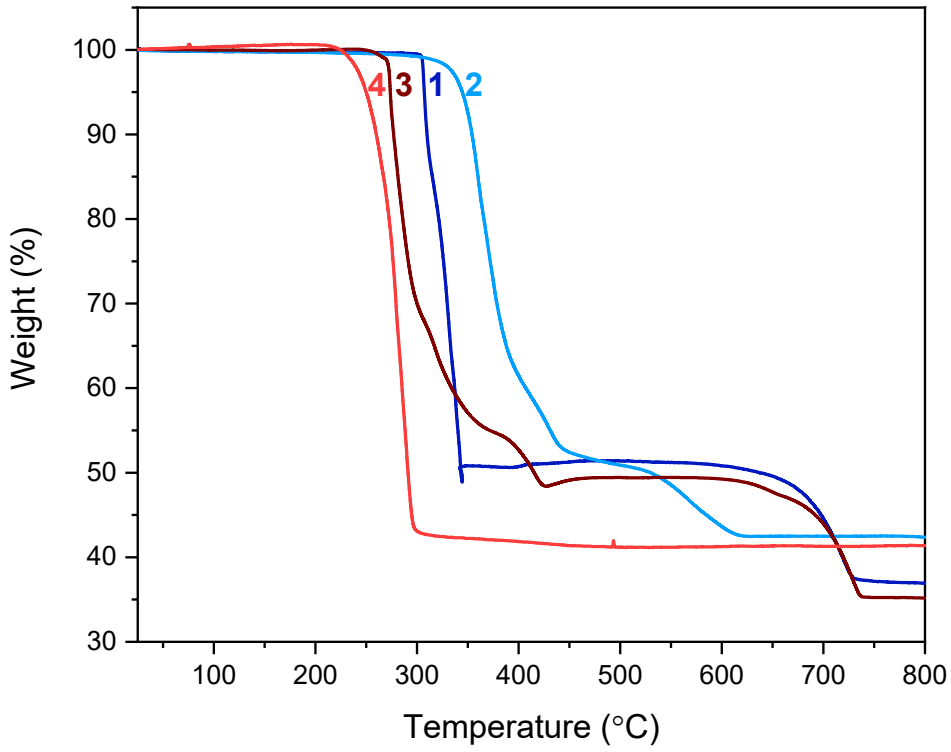

Figure S7. TGA of **1** (dark blue), **2** (blue), **3** (dark red), **4** (red) carried out under air.[15]

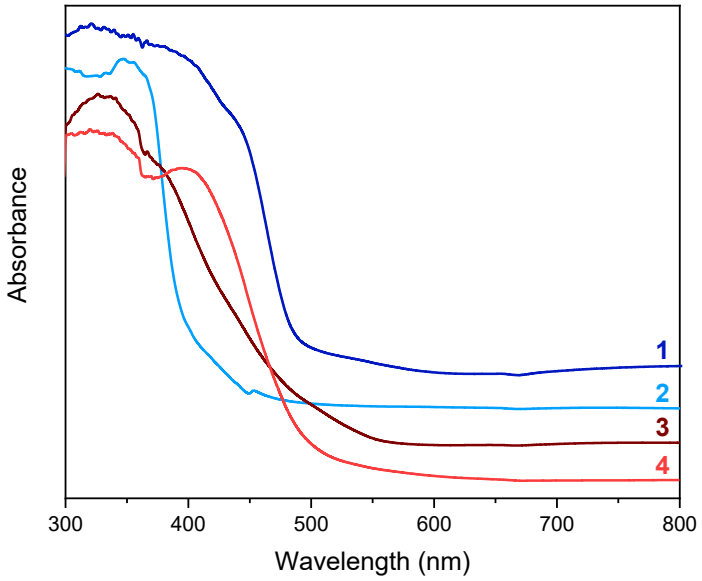

(a)

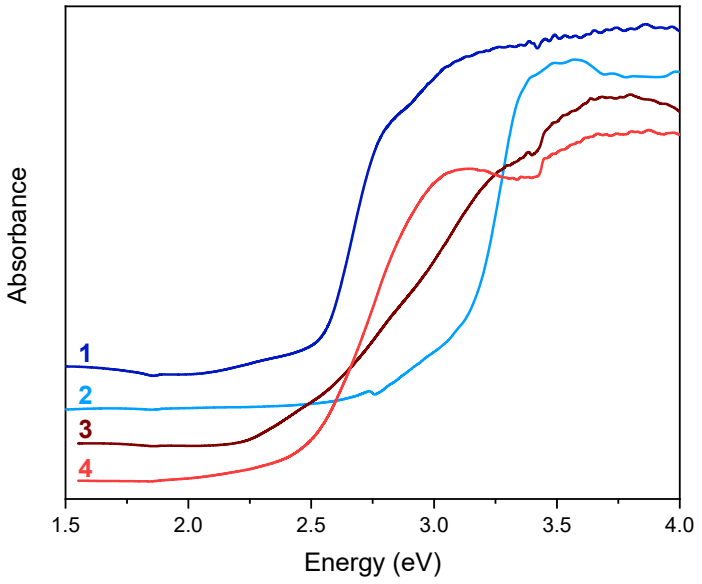

(b)

Figure S8. UV-vis absorption spectra of **1** (dark blue), **2** (blue), **3** (dark red), **4** (red) carried out in solid state at the room temperature as function of (a) wavelength and (b) energy.

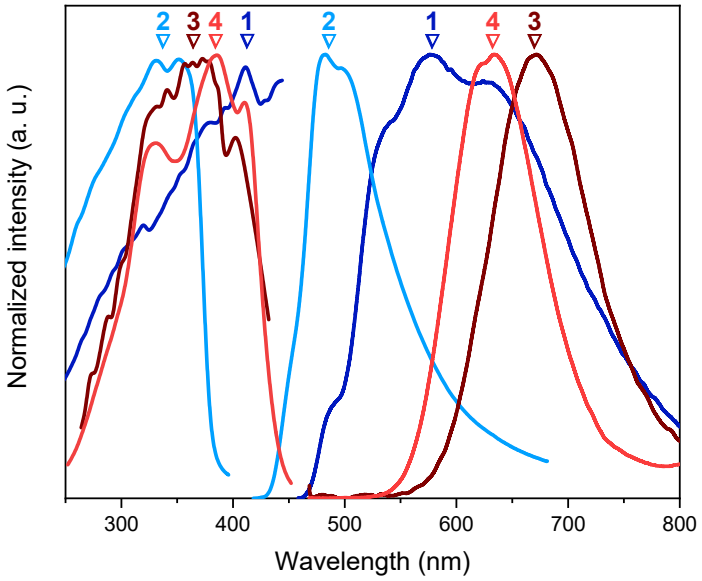

Figure S9. Normalized emission-excitation spectra of **1** (dark blue), **2** (blue), **3** (dark red), **4** (red) carried out in the solid state at 93 K.

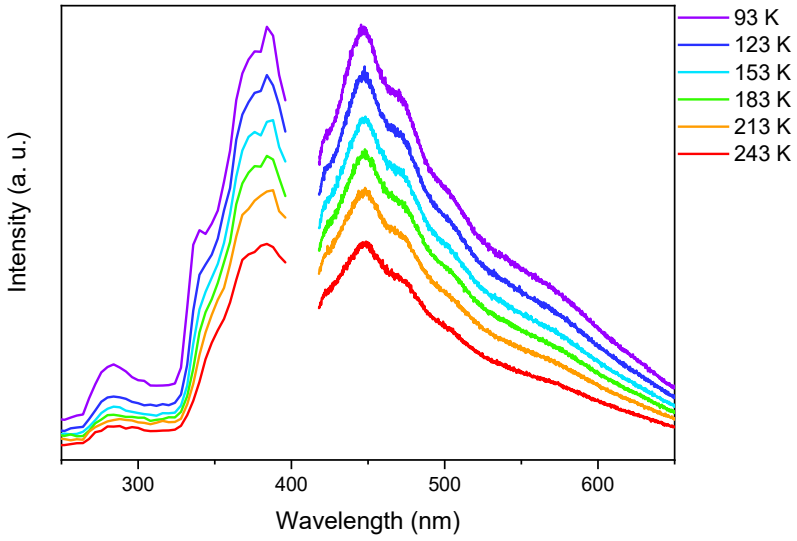

Figure S10. Emission-excitation spectra of *m*-HSPhCO$_2$H carried out in the solid state with temperature.

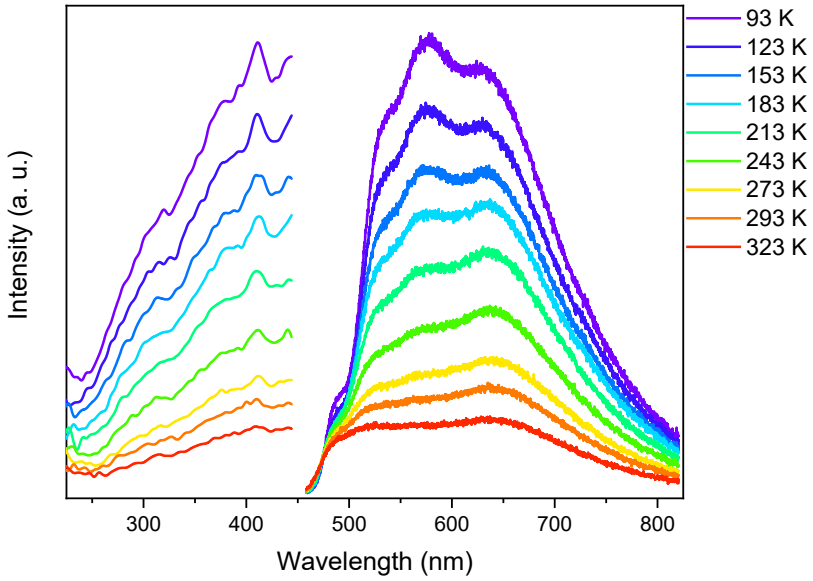

(a)

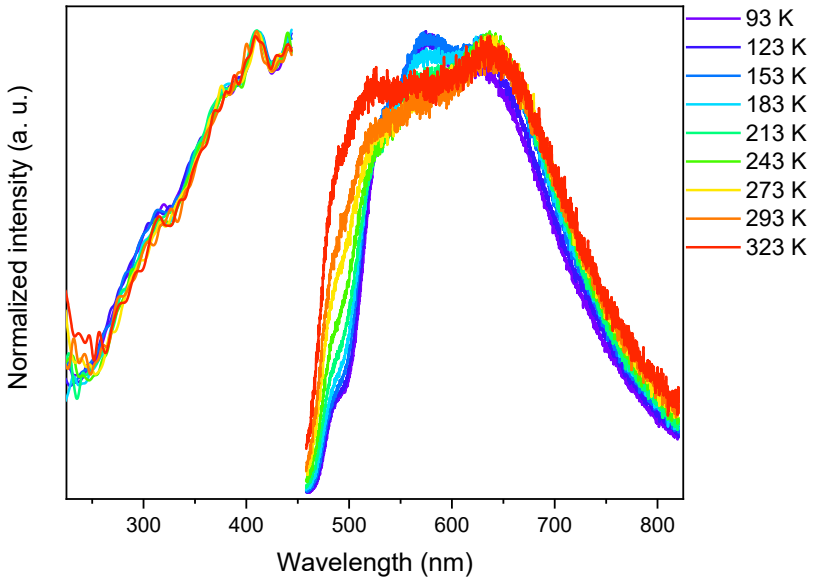

(b)

Figure S11. Change of (a) emission-excitation spectra and (b) normalized emission-excitation spectra of **1** carried out in solid state with temperature.

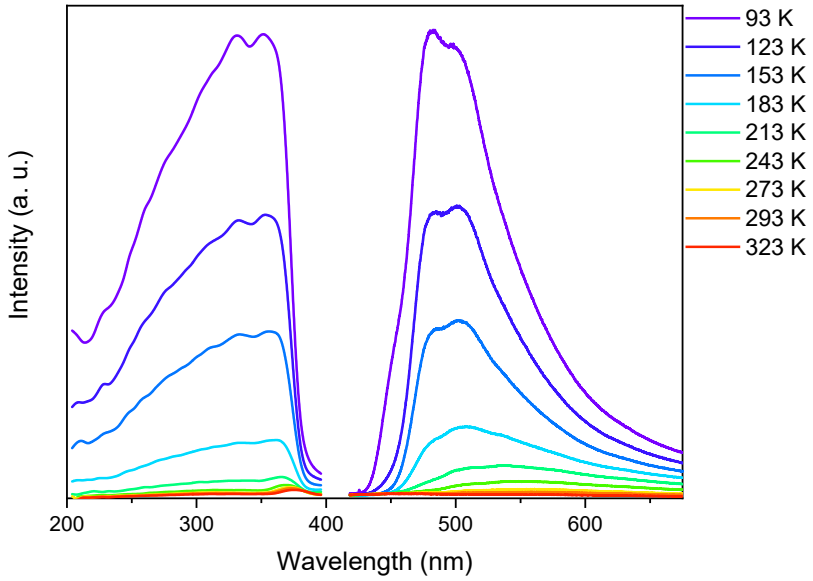

(a)

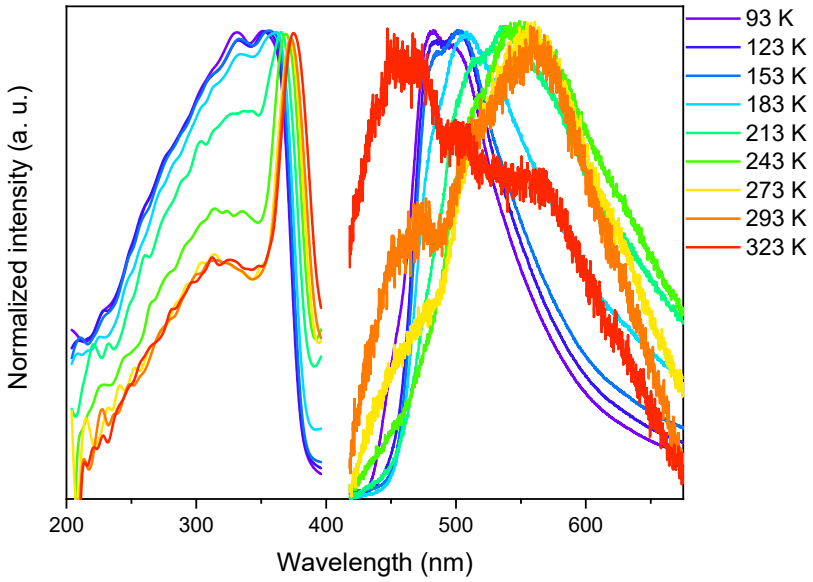

(b)

Figure S12. Change of (a) emission-excitation spectra and (b) normalized emission-excitation spectra of **2** carried out in solid state with temperature.

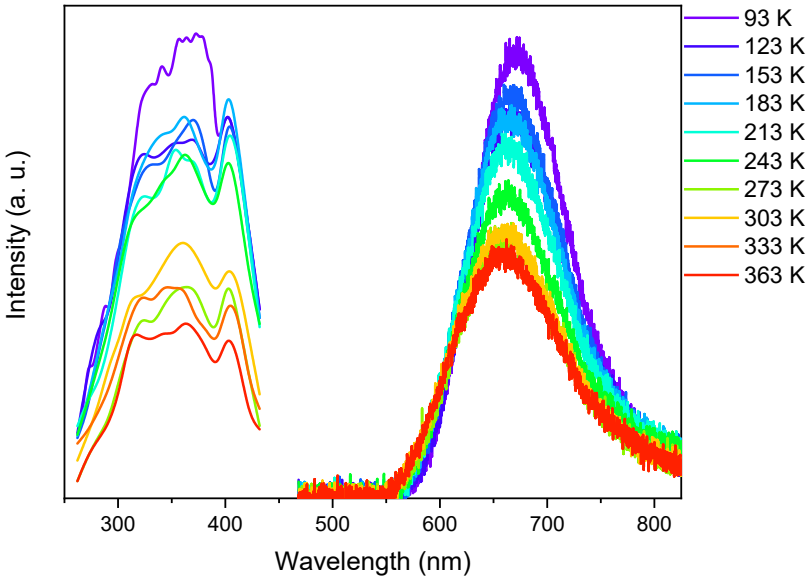

(a)

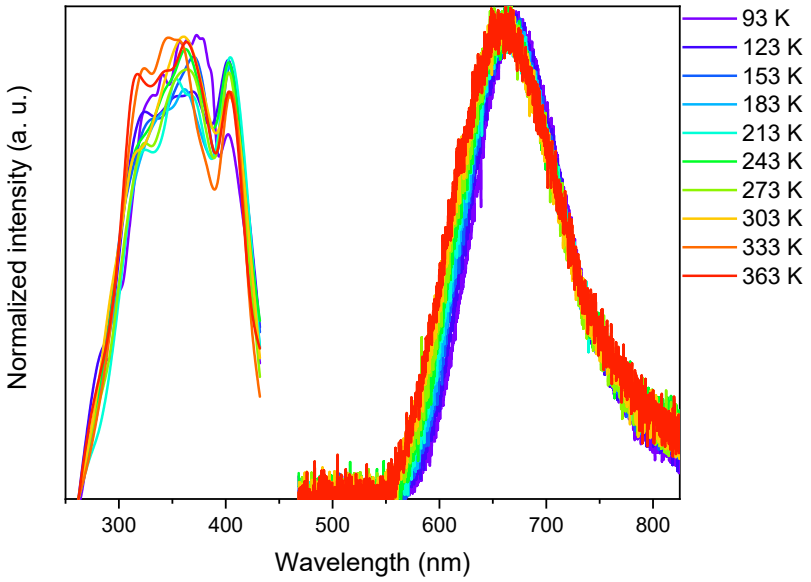

(b)

Figure S13. Change of (a) emission-excitation spectra and (b) normalized emission-excitation spectra of **3** carried out in solid state with temperature.

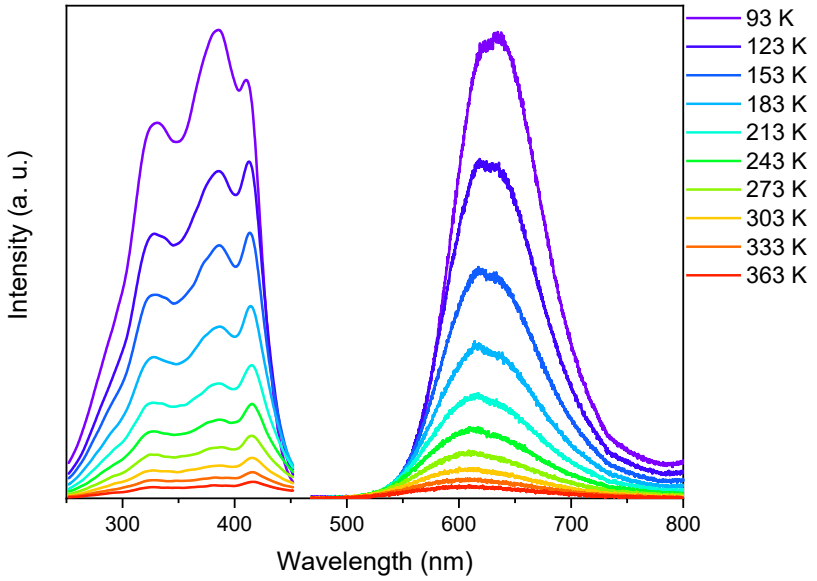

(a)

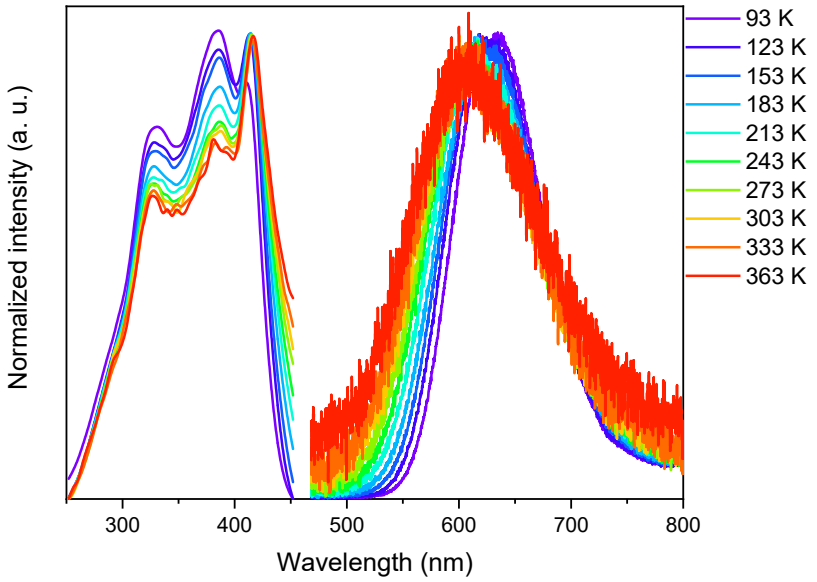

(b)

Figure S14. Change of (a) emission-excitation spectra and (b) normalized emission-excitation spectra of **4** carried out in solid state with temperature.

Table S3. Luminescent mean lifetimes of studied compounds at different temperatures.

	Compound 1	**Compound 2**	**Compound 3**	**Compound 4**
93 K	0.62 µs	2.06 ms	20.00 µs	13.45 µs
183 K	0.30 µs	1.64 ms	11.00 µs	3.01 µs
293 K	0.21 µs			
303 K			2.88 µs	0.26 µs

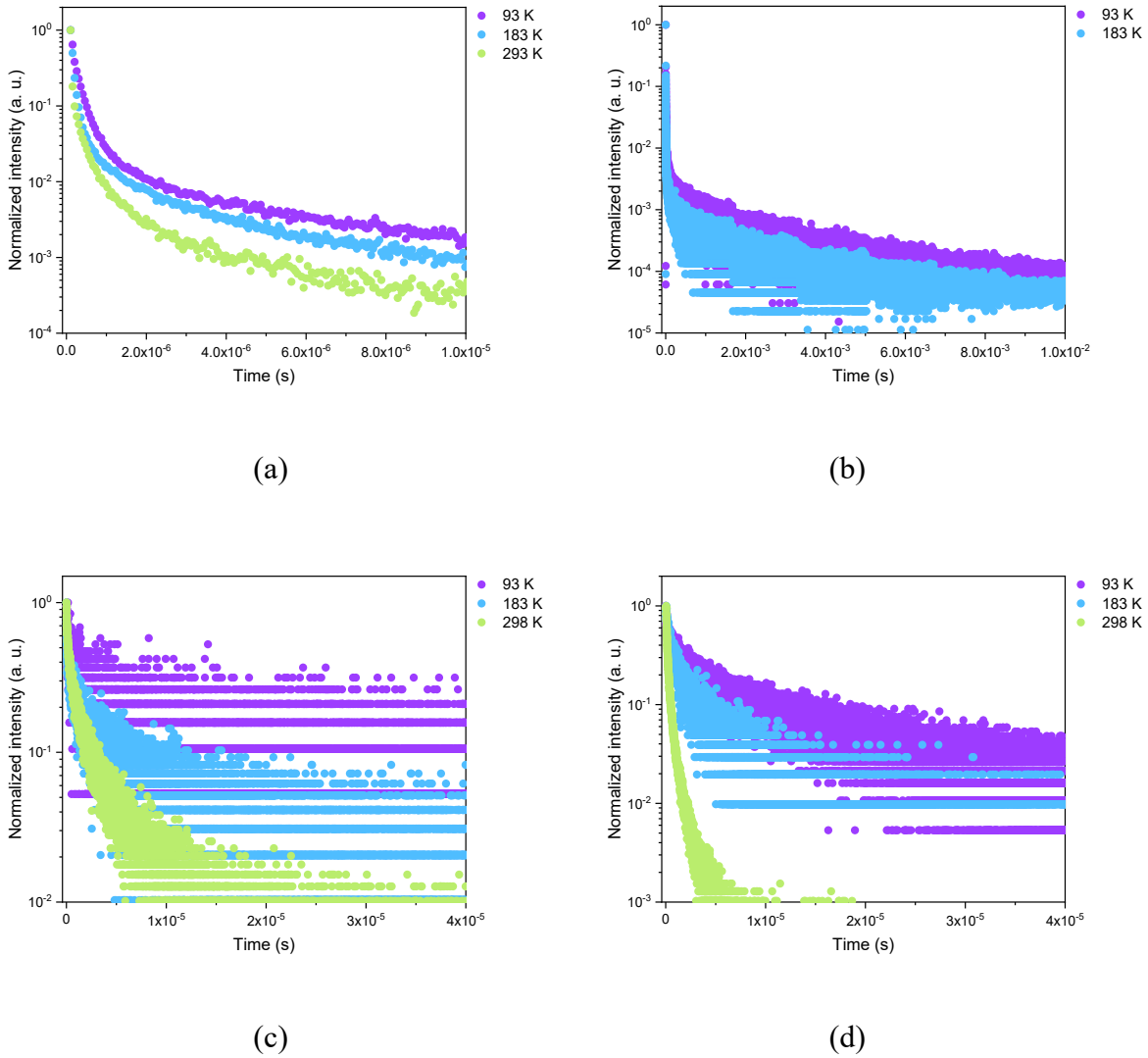

Figure S15. Luminescence lifetime decays of compound (a) **1**, (b) **2**, (c) **3** and (d) **4** carried out in solid-state at different temperatures.

Table S4. Emission peak positions (nm) at 93 K of $[M(x\text{-}SPhCO_2R)]_n$ CPs, *x* = *o*, *m*, *p*, R = H, Me and M= Cu and Ag.

Structure	Compound	Cu	Ref.	Ag	Ref.
2D	$[M(p\text{-}SPhCO_2H)]_n$	500, 660	7	484, 700	8
	$[M(p\text{-}SPhCO_2Me)]_n$	460, 560, 740	11	489, 650	8
	$[M(m\text{-}SPhCO_2H)]_n$	575 (530, 640)^{RT}	This work	482 (460, 555)^{RT}	This work
1D	$[M(m\text{-}SPhCO_2Me)]_n$	670	This work	635	This work
	$[M(o\text{-}SPhCO_2H)]_n$	719	9	654	9
	$[M(o\text{-}SPhCO_2Me)]_n$	610	12	640	12

^{RT} – at room temperature peak splits into two peaks.

References

1. CrysAlisPRO Software system Version 1.171.38.41, *Rigaku Oxford Diffraction*, 2015.
2. J. de Meulenaer and H. Tompa, *Acta Crystallographica*, 1965, **19**, 1014-1018.
3. R. Blessing, *Acta Crystallographica Section A*, 1995, **51**, 33-38.
4. A. Altomare, M. C. Burla, M. Camalli, G. L. Cascarano, C. Giacovazzo, A. Guagliardi, A. Grazia, G. Moliterni, G. Polidori and R. Spagna, *J. Appl. Cryst.*, 1999, **32**, 115-119.
5. P. W. Betteridge, J. R. Carruthers, R. I. Cooper, K. Prout and D. J. Watkin, *J. Appl. Cryst.*, 2003, **36**, 1487.
6. Topas V4.2: General Profile and Structure Analysis Software for Powder Diffraction Data, *Bruker AXS Ltd*, 2008.
7. O. Veselska, L. Cai, D. Podbevšek, G. Ledoux, N. Guillou, G. Pilet, A. Fateeva and A. Demessence, *Inorganic Chemistry*, 2018, **57**, 2736-2743.
8. O. Veselska, C. Dessal, S. Melizi, N. Guillou, D. Podbevšek, G. Ledoux, E. Elkaim, A. Fateeva and A. Demessence, *Inorganic Chemistry*, 2019, **58**, 99-105.
9. O. Veselska, N. Guillou, M. Diaz-Lopez, P. Bordet, G. Ledoux, S. Lebègue, A. Mesbah, A. Fateeva and A. Demessence, *ChemPhotoChem*, 2022, **n/a**, e202200030.
10. K.-H. Low, V. A. L. Roy, S. S.-Y. Chui, S. L.-F. Chan and C.-M. Che, *Chemical Communications*, 2010, **46**, 7328-7330.
11. O. Veselska, D. Podbevšek, G. Ledoux, A. Fateeva and A. Demessence, *Chemical Communications*, 2017, **53**, 12225-12228.
12. A. Abdallah, S. Vaidya, S. Hawila, S.-L. Ornis, G. Nebois, A. Barnet, N. Guillou, A. Fateeva, A. Mesbah, G. Ledoux, A. Bérut, L. Vanel and A. Demessence, *iScience*, 2023, **26**, 106016.
13. M. Baumgartner, H. Schmalle and C. Baerlocher, *J. Solid State Chem.*, 1993, **107**, 63-75.
14. C.-M. Che, C.-H. Li, S. S.-Y. Chui, V. A. L. Roy and K.-H. Low, *Chemistry – A European Journal*, 2008, **14**, 2965-2975.
15. O. Veselska, L. Cai, D. Podbevšek, G. Ledoux, N. Guillou, G. Pilet, A. Fateeva and A. Demessence, *Inorg. Chem.*, 2018, **57**, 2736-2743.